ISSN 1330-3651 (Print), ISSN 1848-6339 (Online)
Received: 12 June 2025; Accepted: 8 September 2025

https://doi.org/10.17559/TV-20250612002742
Original scientific paper

Model Predictive Pitch Control of PMSG-Based WECS Using Fuzzy-MPC and Deep Learning-Based Wind Prediction

S. MUTHARASU*, K. THENMALAR

Abstract: Maintaining steady output power in Wind Energy Conversion Systems (WECS) under varying wind speeds, especially above the rated wind velocity, poses a significant control challenge. To address this, a Model Predictive Control (MPC) approach for pitch angle regulation in WECS is proposed. The nonlinear dynamics of the wind turbine are first linearized and formulated using the Takagi-Sugeno (T-S) fuzzy modelling technique, allowing effective handling of system nonlinearity. The fuzzy-based linearized model is then integrated into the MPC framework, which incorporates both pitch angle and generator torque constraints to ensure safe and optimal turbine operation. To eliminate the reliance on physical wind speed sensors and enhance control performance, a Recurrent Neural Network (RNN) model is developed to predict future wind velocity based on turbine dynamics. This model uses Long Short-Term Memory (LSTM) cells to retain temporal patterns over extended periods, significantly improving the wind speed forecasting accuracy. The integration of this deep learning-based wind prediction into the MPC enhances robustness and adaptability to fluctuating wind conditions. The effectiveness of the proposed predictive pitch angle control strategy is validated on a Permanent Magnet Synchronous Generator (PMSG)-based WECS. Simulation results demonstrate that the proposed method improves power output stability and control responsiveness while reducing mechanical stress on the turbine components. This hybrid approach combining fuzzy modelling, predictive control, and deep learning offers a promising solution for advanced wind turbine control under real-world dynamic conditions.

Keywords: Model Predictive Control (MPC); Recurrent Neural Network (RNN); Takagi-Sugeno Fuzzy Model; Wind Energy Conversion System (WECS)

1 INTRODUCTION

The wind turbine control system is responsible for two key functions. Firstly, it maximizes power extraction during below-rated wind speeds by employing torque control to optimize the turbine's performance [4]. Secondly, when wind speed exceeds the nominal value, the system ensures that the turbine operates at its rated output power by adjusting the blade pitch angle through a pitch control mechanism [5, 6]. In recent years, wind turbines (WTs) are equipped with high capacity up to 20 MW with huge blades due to the wind energy industry's fast expansion. Thus, the large WT has massive structural and fatigue loads, which gives more difficulties to the pitch angle control design task [7].

Consequently, several control principles have been presented to WECSs for the below-rated wind speed region-I control [8, 9]. Most of these techniques rely on three primary methods: Tip Speed Ratio (TSR) Control, Perturbation and Observation (P&O) Method, and Optimal Torque Control (OTC) [10]. In the TSR control scheme, the real-time wind velocity measurement is carried by an anemometer, it leading to complexity in installation and operation [11]. Regarding OTC, it allows maximum power output at any given wind speed. However, its effectiveness becomes substandard for larger wind turbines due to higher inertia, resulting in lower efficiency [12]. The P&O technique is a simple and universal MPPT method, and it requires minimal computational resources and excels in fluctuating wind conditions [1]. However, determining the optimal step size directly impacts its effectiveness [13]. Accordingly, a suitable control scheme can be opted to control the WECSs in the below-rated wind speed range.

Interestingly, many authors focus on the control of WECSs in region-II with the above-rated wind velocity to deliver stable-rated output electricity to the utility grid. In this regard, many pitch angle control strategies are implemented for active power regulation, such as an adaptive robust control [14], intelligent pitch control [15], model predictive control (MPC) [16], reinforcement learning pitch control [17], robust LMI-based pitch controller [18] and sliding mode pitch control [19, 20]. Among various control strategies, MPC methods are frequently employed to maintain the rotor speed and generator output power (P_{out}) at their nominal values during region-II wind speeds.

Moreover, MPC is found to be an advanced process control algorithm that utilizes the system model to forecast the future instant parameters over a prediction horizon. In this, an online optimization is carried across the selected prediction horizon for each of the sampling moments to get the control action [20]. During the last decade, there have been numerous researches that have utilized MPC to construct WT controls. For example, the authors in [20] implemented the nonlinear MPC pitch angle control to avoid flutter of aero elastic instability of the WT blades. However, due to the complicated nonlinear behaviour of the WT dynamics, the traditional nonlinear MPC lacks the performance to linearize the model. The authors in [20] studied multiple MPC to manage P_{out} and reduce the frequent pitch actuation of the WT blades. However, evaluation of such controllers is challenging due to the cross coupling between the region-I and region-II control loops [20]. From the above studies, it has been identified that for developing a model predictive pitch control (MPPC), a linearized pitch actuator model with accurate wind speed information at the selected prediction horizon can have better controllability [2]. In the aspect of linearization, the T-S fuzzy (T-SF) modelling is effective method to deal with the system whose dynamic operating point is changing nonlinearly. For instance, the authors in used the T-S fuzzy system for linearising the nonlinear PMSM. Moreover, the authors in utilized the TS fuzzy method to express the non-linear PMSG-based WECS to several linear arrangements [3].

Besides, the anemometers installed in the WT nacelles measure wind speed. However, their readings are inadequate as they measure the wind speed at specific location rather than measuring it across the entire rotor. For

this reason, replacing mechanical anemometers with a digital wind-speed estimator relying on WECS aerodynamic characteristics is desirable. In this regard, many wind speed estimation methods are developed, like the sensorless effective wind velocity approximation, Kalman filter-based wind speed estimation, and deep neural networks-based wind speed estimation. Among all, DNN is widely recognized for its ability to enable digital processors to automatically learn features from input data and remain robust to parameter changes. Consequently, it is a suitable method for estimating WS.

The foregoing comments make it clear that, enhancing the pitch angle control technique for stable rated output power extraction shows potential for advancement. According to the author's knowledge, minimal research has been conducted on large-scale PMSG-based WECS in this area. Therefore, based on the prior discussed literature review, in this study, we proposed the MPC controller for the PMSG-based WECS pitch angle control. In addition, we introduced a wind speed estimation algorithm using the DNN method. The following summarizes this study's contributions.

1. A deep neural network (DNN) wind speed prediction model is formed by utilizing RNN with a long short-term memory (L-STM) approach.

2. Next, the neural network is trained using the torque, output power, and rotor speed data from WT dynamics without using the wind speed information. By adding L-STM network, the RNN time steps are increased.

3. Furthermore, utilizing the linearized TSF framework of the WECS, an MPPC is designed for pitch angle control with an improved cost function. This approach incorporates data on output power (P_{out}) and R_s constraints.

4. Finally, the proposed control method's effectiveness is validated through comparative results with industrial standard PI and PID control in a 20 MW PMSG-based WECS using MATLAB simulations.

This study's remaining sections are structured as follows: Section 2 details the WT modelling and its T-S fuzzy formulation. Next, Section 3 presents DNN-based WSE method. Then, Section 4 describes the proposed predictive pitch control. Further, the method validations for the proposed WSE method and pitch controller are explained in Section 5. The findings from the research are ultimately presented in Section 6.

2 WIND TURBINE MODELLING

2.1 Rotor Aerodynamic Model

Fig. 1 depicts a PMSG-based WECS's general control framework. Here, the shaft torque T_r and the recorded output power P_m can be shown as follows:

$$\begin{pmatrix} P_m = \frac{1}{2}\rho\pi R^2 V^3 C_p(\beta,\lambda) \\ T_r = \frac{P_m}{\omega_g} \end{pmatrix} \tag{1}$$

where ρ stands for air density, V for WS, R for turbine radius and C_p for WT's power coefficient, and ω_g for generator speed which is dependent on tip speed ratio $\lambda = (\omega_g R)/V$ and pitch angle β, respectively. Also, the WT's power coefficient can be expressed as [20]:

$$C_p(\beta,\lambda) = 0.73\left(\frac{151}{\lambda_j} - 0.5\beta - 0.002\beta^{2.14} - 13.2\right)\cdot \cdot e^{\frac{-18.4}{\lambda_j}} \tag{2}$$

λ_j is given as follows:

$$\frac{1}{\lambda_j} = \frac{1}{\lambda - 0.02\beta} - \frac{0.003}{\beta^3 + 1} \tag{3}$$

As illustrated in Fig.2, the WT operating regions are classified as region-I to region-IV. The C_P and λ relationship with varying β is evident in Fig. 3. The pitch angle enables rapid recovery of the maximum desired output power by adjusting the turbine speed and the orientation of the wind turbine blades, even amid fluctuations in wind speed and direction. Thus, by adjusting the PA, the captured power is kept at the nominal level. The pitch actuator is represented as follows [18]:

$$\beta = -H_n^2\beta - 2\zeta Hn\beta + H_n^2\beta_{(\text{ref})} \tag{4}$$

Here H_n, β_{ref}, and ζ represent natural frequency, pitch angle input, and damping coefficient respectively.

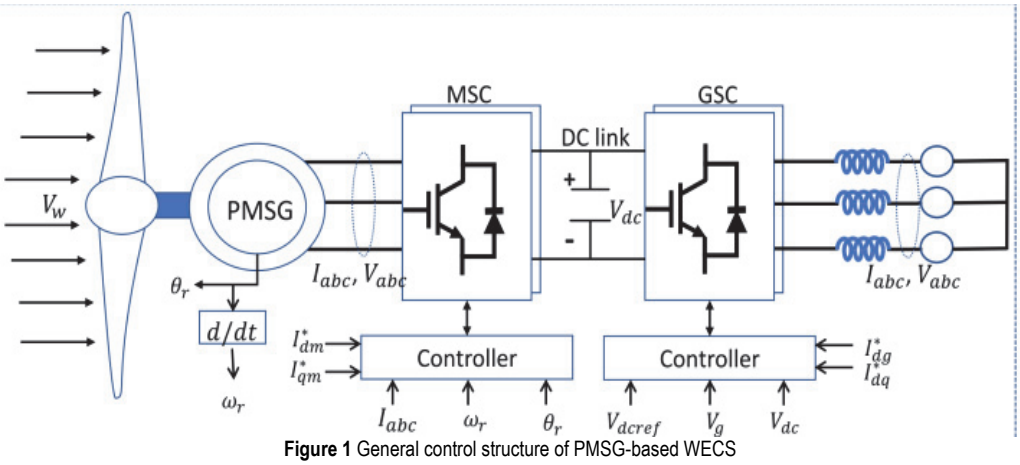

Figure 1 General control structure of PMSG-based WECS

2.1.1 Generator Model

The WT rotor dynamics can be represented in the following way:

$$\omega_g = \frac{T_g}{J} - \frac{T_r}{J} - B_v\,\omega_g \tag{5}$$

where J is the moment of inertia, B_v denotes the frictional coefficient, and T_g represents the generator torque.

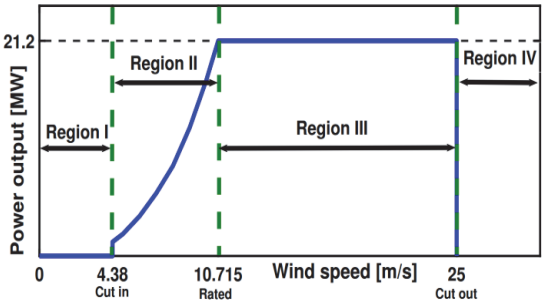

Figure 2 The relationship between a WT output power and windspeed

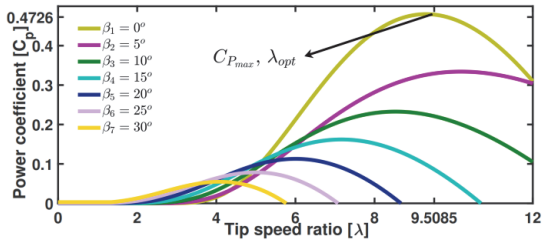

Figure 3 Power coefficient versus tip speed ratio for various pitch angle setting

2.2 Fuzzy Representation of a Wind Turbine

The details of the membership functions used for β and V are summarized in Tab. 1.

Table 1 Membership functions for pitch angle (β) and wind speed (V)

Variable	Range	Membership function	Type
β	[00,300]	Low, Med, High	Triangular
V	[8,26] m/s	Low, Med, High	Gaussian

Consider the state-space model described below:

$$\ddot{x} = A_0\left(x(t)\right)x(t) + B_o\left(x, V\right)$$

$$A_0 = \begin{bmatrix} -B_v & \frac{1}{J} & 0 & 0 \\ 0 & -\frac{1}{\varphi_g} & 0 & 0 \\ 0 & 0 & 0 & 1 \\ 0 & 0 & -H_n^2 & -2\,\zeta H_n \end{bmatrix} \tag{6}$$

$$B_0 = \begin{bmatrix} \frac{T_r}{J} & 0 \\ \frac{1}{\varphi_g} & 0 \\ 0 & 0 \\ 0 & H_n^2 \end{bmatrix}$$

here A and B are the constant matrices with suitable dimensions, $x(t)$ is the states they are in $[\omega_g T_g\ \beta\ \ddot{\beta}\ ]^T$ and the $u(t)$ is the control input. In addition, aerodynamic torque is a nonlinear function that includes pitch angle β, wind speed V, and rotor speed ω_g information. Thus, it can be linearized as follows:

$$T_r = T_{r1}\left(\omega\right)V + T_{r1}\left(\omega\right)\beta + T_{r3}\left(\omega\right)\omega_g \tag{7}$$

and each of its partial derivatives are:

$$T_{r1}\left(x\right)V = \frac{\partial T_r}{\partial V} = \frac{\partial}{\partial V}\left(0.5\rho\pi R^3 V^2\,\frac{C_p\left(\lambda,\beta\right)}{\lambda}\right) \tag{8}$$

$$= 0.5\rho\pi R^3 V\left[2\,\frac{C_p\left(\lambda,\beta\right)}{\lambda} - \lambda\,\frac{\partial\left(\frac{C_p\left(\lambda,\beta\right)}{\lambda}\right)}{\partial\lambda}\right] \tag{9}$$

$$T_{(r2)}\left(x\right) = \left(\frac{\partial T_r}{\partial\beta}0.5\rho\pi R^3 V^2\,\frac{\partial\left(\frac{C_p\left(\lambda,\beta\right)}{\lambda}\right)}{\partial\beta}\right) \tag{10}$$

$$T_{(r3)}\left(x\right) = 0.5\rho\pi R^3\left[\frac{\partial}{\partial\lambda}\frac{C_p\left(\lambda,\beta\right)}{\lambda}\frac{RV^2}{V}\right] \tag{11}$$

$$= 0.5\rho\pi R^4\,\partial\,\frac{C_p\left(\lambda,\beta\right)}{\lambda}V \tag{12}$$

Finally, the WT system (7) includes the linearized aerodynamic torque T_r information from (8). Then, the rearranged dynamics of the WT model is shown by

$$x = Ax\left(t\right)Bu\left(t\right) + B_1\omega\left(t\right) \tag{13}$$

The WT system may need to operate the wind speed up to 26 m/s, which will frequently change. Therefore, we consider the operating range of the variables β and V to vary. In this situation, the nonlinear system (7) is linearized using the T-S fuzzy representation, and it can be illustrated as follows:

$$\left(x\right) = \sum_{(i=1)}^{4} G_{(i)}\left(A_i x\left(t\right) + B_i u\left(t\right) + B_1 i\omega\left(t\right)\right) \tag{14}$$

here the variables β and V bounds are $\beta_1 \le \beta \le \beta_2$ and $V_1 \le V \le V_2$, respectively. And the membership functions are defined as follows:

$$G_2\left(x\right) = H_1^1\left(\beta\right)H_2^2\left(V\right) \tag{15}$$

$$G_3\left(x\right) = H_2^1\left(\beta\right)H_1^2\left(V\right) \tag{16}$$

$$G_4\left(x\right) = H_2^1\left(\beta\right)H_2^2\left(V\right) \tag{17}$$

The membership functions were defined based on the operating limits of β and V as in Tab. 1, and the rule base was constructed using expert knowledge of the WECS dynamics.

3 DNN-BASED WSE

Deep neural networks, such as RNN called L-STM, are being used to estimate wind speed. It can remember long-term dependencies. These deep neural networks can easily identify the patterns in the data sequences. Besides that, they can be suitable for various sensor outputs, images, speeches, stock values, etc. Although traditional RNNs and Gated Recurrent Units (GRUs) are widely used for time-series forecasting, LSTMs were chosen due to their superior ability to capture long-term dependencies in highly nonlinear and volatile signals such as wind speed. Unlike GRUs, LSTMs offer more control through their separate input, forget, and output gates, which improve learning in longer sequences. Empirical studies have also shown that LSTM networks often outperform GRUs in tasks requiring retention of long historical data patterns. The outcome of several stages or layers in history may be "remembered" by this model by applying a feedback loop to the past, making it suited for complicated and long-term relationships characteristic in wind speed data. RNNs retain dynamic long-term temporal contextual information within their hidden layers. The following equation represents the single RNN cell's operation:

$$h_t = \tanh\left(W\left[L_{t-1}, x_t\right] + b\right) \tag{18}$$

where W, b, h_t and L_{t-1} are represented as the weight matrix, bias matrix, hidden state at current time-step and past time-step. In addition, the primary operations of an LSTM network are represented as follows. The "forget gate function" f_t represents which pieces of information are to be removed from the cell state following the most recent hidden state, L_{t-1}, and the latest input x_t:

$$f_t = \Phi\left(W_f\left[L_{t-1}, x_t\right] + b_f\right) \tag{19}$$

where the cell's input and output vectors are x_t and L_{t-1} respectively. Input applied weights are represented by the W_f, b_f and Φ denotes the bias vector and sigmoid function, respectively. The second step is choosing the information that should be gathered in the cell state. It has been divided into two halves, the latest cell state, C_t, has been formed. The input gate i_t will scale new candidate cell state.

$$i_t = \Phi\left(W_i\left[L_{t-1}, x_t\right] + b_i\right) \tag{20}$$

where L_{t-1} and x_t denote the last hidden state and the latest input, respectively. W_c and W_i are denoting weight matrices. The tanh() function represents the sigmoid tangent, while Φ() denotes the hyperbolic tangent function.

In the third step, the new cell state C_t has been upgraded, merging the past cell state C_{t-1} and the latest cell state C_t. Moreover, the past cell state is influenced by the "forgetgate" f_t which is then scaled using the input gate

$$i_t, \overline{C_t} = f_t\, x\, C_{t-1} + i_t\, x C_t \tag{21}$$

In the end, the output function splits into two steps. First, the latest gate, termed the output gate O_t, is used to choose which elements of the cell state should be produced. The second one is desired output. Here, the cell state is activated using the tanh function and filtered by multiplying the output function.

4 MODEL-BASED PREDICTIVE PITCH CONTROL STRATEGY (MPPC)

MPPC is extensively applied in industrial settings because of its exceptional capability to address control challenges by managing system variables with constraints [19]. The core parts of the proposed MPPC is the predictor, optimization solver and state estimator.

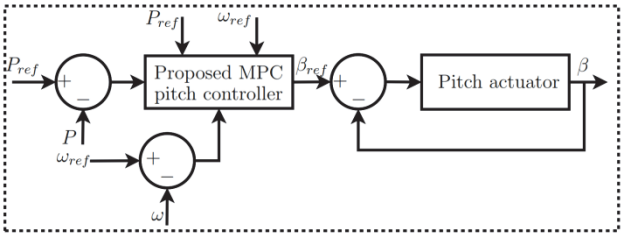

Figure 4 Structure of cascade forward back-propagation neural network

The Fig.4 represents the schematic diagram of the proposed pitch angle control system based on MPC. The controller utilizes Eq. (13) to forecast the output over a specified prediction window. The estimated future states at time step k are:

$$\begin{aligned} x(k+n) &= A^n x(k) + A^{(n-1)} B u(k) + A^{(n-1)} B_1 \omega(t) + \\ &+ A^{(n-2)} B u(k+1) + A^{(n-2)} B_1 \omega(t) + B u(k+n-1) + \\ &+ B_1 \omega(t) \end{aligned} \tag{22}$$

where $x(k)$ signifies the present state, $x(k + n)$ denotes the predicted value of the n-step at sample k, and k is the current sampling interval. A, B and B_1 are $\sum_{i=1}^{4} G_i A_i$, $\sum_{i=1}^{4} G_i B_i$ and $\sum_{i=1}^{4} G_i B_{1i}$, respectively. The upcoming control inputs are represented as $u(k)$, $u(k + 1)$, $u(k + n - 1)$. Moreover, $y(k + n)$ denotes the predicted output n-th steps given data at the sample k. The predicted output can be defined. Then, the traditional cost function's goal is to minimise the pitch actuation error during the subsequent switching time. Hence, the traditional cost function is represented as follows [17, 20]:

$$j(k) = \sum_{i=H_w}^{H_P} x\left(k+i \vdots k\right)^2 + \sum_{(i=0)}^{(H_u-1)} \vdots\vdots x\left(k+i \vdots k\right) \vdots\vdots^2 \tag{23}$$

where the H_p denotes the prediction, H_u denotes control horizon. Assume that H_u is less than or equal to H_p.$\Delta_u(k + i) = 0$ for $i \geq H_u$. Considering this cost function (21), it only depends on the output of the WT power in the instant k and the respective times. As a result, a parameter or sensing

error, a steady-state error, may be produced in the system during the high wind speed regions.

To effectively control the pitch angle in WECS during the above-rated WS, the control system tries to decrease control effort while minimizing power discrepancies and rotor speed. The proposed MPPC should optimise R_s and power to accomplish the control aim. In this regard, the constraints of R_s, pitch angle and P_{out} are included in the proposed cost function. Additionally, the proposed cost function minimizes deviations of the predicted controlled output $y(k + n)$ from the reference trajectory. The proposed cost function is described as follows.

$$\begin{cases} j(k) = \sum_{i=0}^{\infty} \vdots\vdots y(k+i \vdots k) - r(k+i) \vdots\vdots^2 \end{cases} \quad (24)$$

where $G_P(k) = P^*(k + 1) - P^q(k + 1) \in (P^*(k + 1) - P^q(k + 1))$ and $G_\omega(k) = \omega_g^*(k + 1) - \omega_g^P(k + 1) \in (\omega_g^*(k + 1) - \omega_g^P(k + 1))$. ω_g^* and $P^*$the rotor speed and the power references. $\omega_g^*$and P^*denote the filtered speed and power references. Moreover, super script p and q indicate speed and power predicted values, respectively. The constraints on the PA's fluctuation are detailed below.

$$\begin{aligned} &\{\| u(k+i \,|k) \| \leq \beta_{\max} i \geq 0, \\ &\{\| \Delta u(k+i \,|k) \| \leq \beta_{\max} i \geq 0, \\ &\{\| y(k+i \,|k) \| \leq y_{\max} i \geq 0, \end{aligned} \quad (25)$$

where $\beta_{\max}$ and $\Delta\beta_{\max}$ indicate the maximum pitch angle and rate of change. $y_{\max}$ denotes the maximum output. Finally, based on T-SF paradigm, the Kalman filter (KF) is implemented to measure some immeasurable states. The stochastic form of KF is given as follows:

$$x(k+1) = Ax(k) + Bu(k) + v(k) \quad (26)$$

$$y(k) = cx(k) + \delta(k) \quad (27)$$

where A, B and C denote the constant matrices. v and δ denote stochastic signals. The covariance of v and δ are defined as:

$$\Xi v(k) v(\Phi)^T = Q\delta(k - \tau) \quad (28)$$

where $\delta(k - \tau) = 1$ if $k = \tau$ and $\delta(k - \tau) = 0$ else, Ξ is the expectation operator. Q and R are the positive semi-definite and positive definite, respectively. The need of KF is to determine $\hat{x}(k)$ of $x(k)$. Also the covariance of the state estimation error is reduced. The fuzzy rules and the membership function determine the state estimation.

Rule i: If the wind speed is Vj, then

$$x(k+1) = A_j x(k) + B_j U(k) + K_j \left(y(k) - C_j x(k) \right) \quad (28)$$

where j and K_j represent the rule index and Kalman gain, respectively.

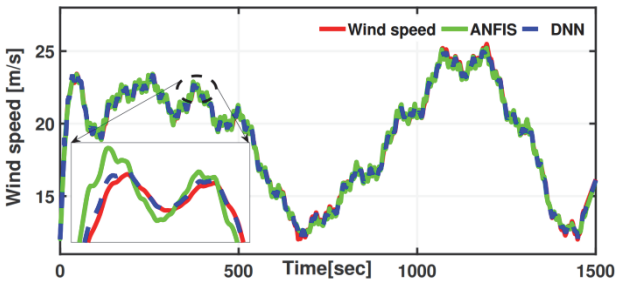

Figure 5 Actual vs. estimated wind speeds using ANFIS and DNN

5 METHOD VALIDATION

The suggested approach's efficiency is assessed using MATLAB simulations using a 20 MW PMSG-based WECS setup. Initially, a randomly fluctuating wind speed is applied and compared with the ANFIS method to validate accurate WSE. Subsequently, both stepwise and randomly varying wind speed is utilized to evaluate the performance of the recommended MPPC. In addition, it is compared with the standard PI and PID controllers to show the superiority of the suggested control methods. The WT and the PMSG specifications are mentioned in Tab. 2 and Tab. 3, respectively.

Table 2 PMSG-Based WECS-Mechanical Parameters

Specifications	Value [unit]
Rated wind speed	10.7145 m/s
Power coefficient	0.4730
Rated mechanical power	21.20 MW
Rated rotor speed	7 rpm
Tip speed ratio	9.509
Blade radius	137.9 m

The wind profile was designed to reflect realistic wind conditions for large-scale turbines. A randomly varying wind speed profile was used ranging from 12 m/s to 25 m/s, generated using a Gaussian process with a standard deviation of 3.5 m/s and a mean of 18 m/s. For step response evaluation, transitions occurred at t = 200 s, 400 s, 800 s, and 1000 s. The PMSG-based WECS was modeled in MATLAB/Simulink using the mechanical and electrical parameters listed in Tab. 1 and Tab. 2. The pitch actuator was modeled with a natural frequency of 0.3 Hz and a damping ratio of 0.6. The sampling time for the MPC loop was set to 0.1 s, with a prediction horizon of 15 steps and a control horizon of 5 steps.

Table 3 Electrical Specifications of the PMSG-WECS

Specifications	Value [unit]
Rated output power	20 MW
Rated generator speed	7.1567 rpm
Rated generator torque	28.2754 MNm
Output line voltage	6.9 kV
Generator efficiency	94%

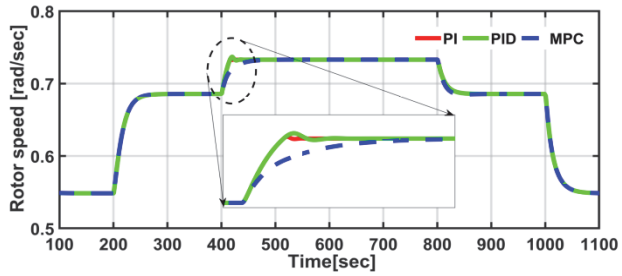

Figure 6 Rotor speed response for state varying wind velocity

5.1 Effective WSE

In this investigation, a randomly varying wind velocity is considered to verify the applicability of the recommended DNN. The wind profile varies between 12 m/s to 25 m/s for the duration of 1500 seconds. The shaft speed, torque, and output power data were numerically calculated and utilised to train the deep neural network. From the calculated dataset, 15% of data are used for training and the other 15% for testing purposes. From Tab. 4 and Tab. 5, it can be observed that the proposed method demonstrates improved accuracy and robustness compared to ANFIS.

Table 4 MSE of proposed method and the ANFIS

Methods	MSE	RMSE	MAE
DNN	0.0147	0.1212	0.0935
ANFIS	0.1690	0.4110	0.3087

Table 5 Performance evaluation utilizing step wind speed

Control methods	Overshoot / MW	Steady state error / MW	Settling time / Sec
PI	0.0097704	0.0022801	22
PID	0.0319890	0.0022900	33
MPC	0.0125500	0.0015290	3

5.2 Proposed Pitch Controller with Step Wind Speed

A step wind profile is employed to verify the suggested MPPC through simulation. The wind speed initially increases from 8 m/s to 10 m/sat t = 200 seconds, followed by an increase to 11 m/s at 400 seconds, reaching above-rated velocity. Subsequently, it drops from 11 m/s to 10 m/s at 800 seconds and further decreases to 8 m/s at 1000 seconds. The performance of the PMSG-based WECS with the proposed MPPC is assessed over duration of 1100 seconds using these step variations in wind speed. Additionally, its effectiveness is contrasted with conventional PI and PID controllers. The rotor speed response shows that all control methods track the desired speed effectively. However, at 400 sec, the wind velocity suddenly increased above the rated WS; at this time, the proposed MPPC method effectively manipulates the pitch actuation and leads to smoother speed tracking to the rated rotor speed. It greatly suppresses the high frequency speed oscillations when the wind speed exceeds the rated wind speed, as mentioned in an enlarged picture in Fig. 7. It will greatly help to reduce the mechanical stress on the WT when wind speed is suddenly increased to an above-rated wind speed. In addition to MSE, the proposed DNN model achieved an RMSE of 0.1212 and MAE of 0.0935, indicating superior predictive accuracy over the ANFIS model (RMSE = 0.4110, MAE = 0.3087) as in Tab. 4. The power coefficient remains at its maximum C_p value if wind speed < rated level. Once wind speed surpasses the rated threshold, the pitch control mechanism is activated to regulate the wind turbine's optimal R_s and P_{out}. In addition, the output power overshoot, steady state error, and settling time calculated at 400s (above-rated wind speed) analyze the efficacy of the suggested pitch control over the PI and PID control methods. The proposed MPPC method outperformed PI and PID control methods. From the above findings, the performance of the WT is improved while employing the proposed MPPC method. As a result, the output power extracted has been more stabilized at the rated value with minimum mechanical stress on the wind turbine blades.

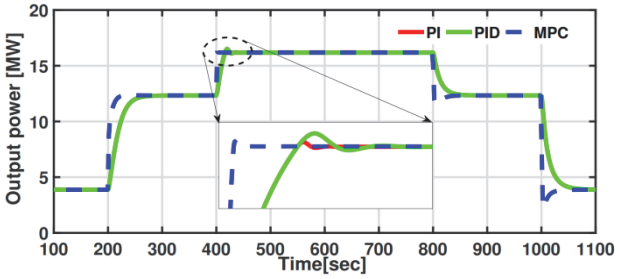

Figure 7 Extracted aerodynamic power

5.3 Proposed Pitch Controller Responses with Randomly Varying WS

The dynamic efficacy of the presented MPPC strategy is assessed in a PMSG-based WECS under randomly fluctuating wind conditions. Additionally, its effectiveness is compared with conventional PI and PID controllers. The estimated WS, obtained from the DNN output, is used to validate the proposed MPC algorithm. The wind speed ranges from 12 to 25 m/s, exceeding the rated velocity of the wind turbine. Simulation results of the WT responses under randomly varying wind speed with the proposed and conventional control methods are presented. Using the proposed MPPC, pitch angle remains stable with minimal fluctuations and reduced pitch adjustments at above-rated wind speeds. The results in Tab. 6 highlight the effect of random wind speed on maximum power oscillation.

Table 6 Maximum power oscillation under random wind speed

Control methods	Power oscillation / MW
PI	0.00651
PID	0.00675
MPC	0.00159

5.4 Comparative Discussion with Conventional MPC Approaches, Real-time Implementation and Computational Cost

Traditional linear MPC approaches typically rely on fixed linear models derived at a nominal operating point. These methods lack adaptability when applied to large-scale nonlinear systems such as wind turbines operating under fluctuating wind conditions. In contrast, the proposed fuzzy-MPC model incorporates a Takagi-Sugeno fuzzy system to manage nonlinearities and model variations more effectively. Moreover, by integrating LSTM-based wind prediction, the control strategy benefits from enhanced future state estimation, reducing prediction mismatch. Unlike conventional MPCs that assume measured wind speed inputs, this method eliminates dependency on physical wind sensors while maintaining better power regulation and rotor speed tracking.

The proposed control algorithm was tested using MATLAB on a standard PC with an Intel Core i7 processor. Each control cycle required approximately 6-8 milliseconds, well within real-time feasibility for a sampling time of 100 ms. Although the addition of fuzzy modeling and LSTM-based wind estimation slightly increases computational complexity, the modular structure

allows for parallel execution on real-time hardware such as dSPACE or OPAL-RT platforms. Moreover, modern wind turbine controllers often have sufficient onboard computational resources to accommodate such hybrid MPC structures. Future work will explore hardware-in-the-loop (HIL) implementation to validate real-time performance under embedded constraints.

6 CONCLUSION

This study proposed an advanced predictive pitch control strategy for a 20 MW Permanent Magnet Synchronous Generator (PMSG)-based WECS, aiming to improve power stability and control robustness under varying wind conditions. The Takagi-Sugeno Fuzzy (T-SF) linearization framework was first applied to model the nonlinear dynamics of the WECS, enabling a simplified yet accurate representation suitable for predictive control implementation. A Deep Neural Network (DNN) integrated with Long Short-Term Memory (LSTM) architecture was introduced to accurately estimate wind velocity, thereby eliminating the need for physical wind speed sensors. This predictive capability significantly enhanced the responsiveness and adaptability of the control system. Based on the linearized model and wind estimation, a Model Predictive Control (MPC) scheme was formulated to manage pitch angle adjustments while explicitly considering system constraints such as pitch rate limits and mechanical bounds. In addition, a Kalman Filter (KF) was employed to estimate internal states that are not directly measurable, further enhancing the reliability of the control system. The complete control framework was validated through detailed simulations using the dynamic parameters of a 20 MW PMSG-based WECS. Comparative analyses were performed against conventional Proportional-Integral (PI) and Proportional-Integral-Derivative (PID) controllers. The simulation results demonstrated that the proposed MPC-based pitch control strategy, supported by deep learning-based wind prediction and state estimation, outperformed traditional methods in terms of response time, power stability and system efficiency. Overall, the integrated control approach shows promise for real-time wind turbine applications, particularly in large-scale WECS installations.

7 REFERENCES

[1] Palani, A., Mahendran, V., Vengada Krishnan, K., Muthusamy, S., Mishra, O. P., Ramamoorthi, P., Maurya, M. R., & Sadasivuni, K. K. (2024). A novel design and development of multilevel inverters for parallel operated PMSG-based standalone wind energy conversion systems. *Iranian Journal of Science and Technology, Transactions of Electrical Engineering*, *48*(1), 277-287. https://doi.org/10.1007/s40998-023-00661-2

[2] Zhang, Z., Zhao, Y., Qiao, W., & Qu, L. (2015). A discrete-time direct torque control for direct-drive PMSG-based wind energy conversion systems. *IEEE Transactions on Industry Applications*, *51*(4), 3504-3514. https://doi.org/10.1109/TIA.2015.2413760

[3] Meghni, B., Ouada, M., & Saad, S. (2020). A novel improved variable-step-size P&O MPPT method and effective supervisory controller to extend optimal energy management in hybrid wind turbine. *Electrical Engineering*, *102*(2), 763-778. https://doi.org/10.1007/s00202-019-00911-9

[4] Bagheri, P., Behjat, L., & Sun, Q. (2022). Nonlinear control of a class of non-affine variable-speed and variable-pitch wind turbines with radial-basis function neural networks. *ISA Transactions*, *131*, 197-209. https://doi.org/10.1016/j.isatra.2022.05.004

[5] Jia, C., Wang, L., Meng, E., Chen, L., Liu, Y., Jia, W., Bao, Y., & Liu, Z. (2021). Combining LIDAR and LADRC for intelligent pitch control of wind turbines. *Renewable Energy*, *169*, 1091-1105. https://doi.org/10.1016/j.renene.2021.01.055

[6] Bououden, S., Chadli, M., Filali, S., & El Hajjaji, A. (2016). Fuzzy model based multivariable predictive control of variable speed wind turbines. *Renewable and Sustainable Energy Reviews*, *55*, 957-970. https://doi.org/10.1016/j.rser.2015.11.065

[7] Meng, W., Yang, Q., Ying, Y., Sun, Y., Yang, Z., & Sun, Y. (2013). Adaptive power capture control of variable-speed wind energy conversion systems with guaranteed transient and steady-state performance. *IEEE Transactions on Energy Conversion*, *28*(3), 716-725. https://doi.org/10.1109/TEC.2013.2273357

[8] Jiao, X., Yang, Q., & Xu, B. (2021). Hybrid intelligent feedforward-feedback pitch control for VSWT with predicted wind speed. *IEEE Transactions on Energy Conversion*, *36*(4), 2770-2781. https://doi.org/10.1109/TEC.2021.3076839

[9] Lin, Z., Chen, Z., Wu, Q., Yang, S., & Meng, H. (2018). Coordinated pitch & torque control of large-scale wind turbine based on Pareto efficiency analysis. *Energy*, 147, 812-825. https://doi.org/10.1016/j.energy.2018.01.120

[10] Abdullah, M. A., Yatim, A., Tan, C. W., & Saidur, R. (2012). A review of maximum power point tracking algorithms for wind energy systems. *Renewable and Sustainable Energy Reviews*, *16*(5), 3220-3227. https://doi.org/10.1016/j.rser.2012.02.016

[11] Wang, L., Cao, L., & Zhao, L. (2018). Non-linear tip speed ratio cascade control for variable speed high power wind turbines: a backstepping approach. *IET Renewable Power Generation*, *12*(8), 968-972. https://doi.org/10.1049/iet-rpg.2017.0698

[12] Srinivasan, T., Wang, X., Kim, H. J. et al. (2021). Performance Enhancement for Microgrids Under the Demand Uncertainties with the Presence of Multiple DGs Through Stochastic Ranking Algorithm. *Journal of Electrical Engineering & Technology*, *16*, 223-238. https://doi.org/10.1007/s42835-020-00602-7

[13] Nasiri, M., Milimonfared, J., & Fathi, S. (2014). Modeling, analysis and comparison of TSR and OTC methods for MPPT and power smoothing in permanent magnet synchronous generator-based wind turbines. *Energy Conversion and Management*, *86*, 892-900. https://doi.org/10.1016/j.enconman.2014.06.047

[14] Venkateswaran, R., Natesan, B., Lee, S. R., & Joo, Y. H. (2022). Maximum power extraction for PMSG-based WECS using Q-learning MPPT algorithm with finite-time control scheme. *IEEE Transactions on Sustainable Energy*, *14*(1), 516-524. https://doi.org/10.1109/TSTE.2022.3218045

[15] Sierra-Garcia, J. E., Santos, M., & Pandit, R. (2022). Wind turbine pitch reinforcement learning control improved by PID regulator and learning observer. *Engineering Applications of Artificial Intelligence*, *111*,104769. https://doi.org/10.1016/j.engappai.2022.104769

[16] Hassan, H., ElShafei, A., Farag, W., & Saad, M. (2012). A robust LMI-based pitch controller for large wind turbines. *Renewable Energy*, *44*, 63-71. https://doi.org/10.1016/j.renene.2012.01.092

[17] Colombo, L., Corradini, M. L., Ippoliti, G., & Orlando, G. (2020). Pitch angle control of a wind turbine operating above the rated wind speed: A sliding mode control approach. *ISA Transactions*, *96*, 95-102. https://doi.org/10.1016/j.isatra.2019.06.021

[18] Yin, X., Zhang, W., Jiang, Z., & Pan, L. (2019). Adaptive robust integral sliding mode pitch angle control of an electro-hydraulic servo pitch system for wind turbine. *Mechanical Systems and Signal Processing*, *133*, 105704. https://doi.org/10.1016/j.ymssp.2019.05.038

[19] Ghouraf, D. E. (2023). An advanced control applied to PMSG wind energy conversion system implemented under graphical user interface. *Electrical Engineering*, *105*(6), 3841-3852. https://doi.org/10.1007/s00202-023-01885-5

[20] Mohamed Shuaib, Y., Surya Kalavathi, M., & Asir Rajan, C. C. (2014), Optimal Reconfiguration in Radial Distribution System Using Gravitational Search Algorithm. *Electric Power Components and Systems*, *42*, 703-715. https://doi.org/10.1080/15325008.2014.890971

Contact information:

S. MUTHARASU, Assistant Professor
(Corresponding Author)
Department of EEE,
Vivekanandha College of Engineering for Women,
Tiruchengode, Tamil Nadu, India
E-mail: smutharasu12@gmail.com

K. THENMALAR, Professor
Department of EEE,
Vivekanandha College of Engineering for Women (Autonomous),
Tiruchengode, Tamil Nadu, India
E-mail: thenmalark@gmail.com